

AU-A139 058

REDOX THERMODYNAMICS OF SURFACE-BOUND REACTANTS  
ILLUSTRATIVE BEHAVIOR OF... (U) PURDUE UNIV LAFAYETTE IN  
DEPT OF CHEMISTRY J T HUPP ET AL. NOV 83 TR-18

1/1

UNCLASSIFIED

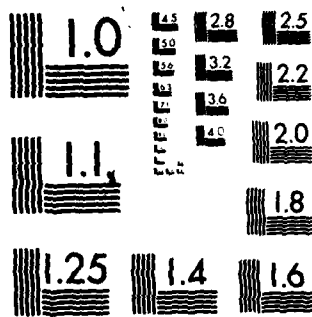
N00014-79-C-0670

F/G 7/4

NL



END  
PAGE  
FILMED  
4-24  
DTIC



MICROCOPY RESOLUTION TEST CHART  
NATIONAL BUREAU OF STANDARDS-1963-A

10

OFFICE OF NAVAL RESEARCH  
Contract N00014-79-C-0670

TECHNICAL REPORT NO. 18

Redox Thermodynamics of Surface-Bound Reactants.  
Illustrative Behavior of Cobalt(III)/(II)  
Macrobicyclic "Cage" Complexes

by

J. T. Hupp, P. A. Lay, H. Y. Liu, W. H. F. Petri

A. M. Sargeson and M. J. Weaver

Prepared for Publication

in the

Journal of Electroanalytical Chemistry

Department of Chemistry

Purdue University

West Lafayette, IN 47907

November 1983

Reproduction in whole or in part is permitted for  
any purpose of the United States Government

This document has been approved for public release  
and sale; its distribution is unlimited

Distribution for	
By	
Distribution	
Approved for Release	
Dist	
A-1	

DTIC  
SELECTED  
MAR 13 1984  
E

AD A139058

DTIC FILE COPY

84 03 15 174

REPORT DOCUMENTATION PAGE		READ INSTRUCTIONS BEFORE COMPLETING FORM
1. REPORT NUMBER Technical Report No. 18	2. GOVT ACCESSION NO. AD-A139058	3. RECIPIENT'S CATALOG NUMBER
4. TITLE (and Subtitle) Redox Thermodynamics of Surface-Bound Reactants. Illustrative Behavior of Cobalt(III)/(II) Macro- bicyclic "Cage" Complexes		5. TYPE OF REPORT & PERIOD COVERED Technical Report No. 18
7. AUTHOR(s) J. T. Hupp, P. A. Lay, H. Y. Liu, W. H. F. Petri A. M. Sargeson and M. J. Weaver		6. PERFORMING ORG. REPORT NUMBER
9. PERFORMING ORGANIZATION NAME AND ADDRESS Department of Chemistry Purdue University West Lafayette, IN 47907		8. CONTRACT OR GRANT NUMBER(s) N00014-79-C-0670
11. CONTROLLING OFFICE NAME AND ADDRESS Office of Naval Research Department of the Navy Arlington, VA 22217		10. PROGRAM ELEMENT, PROJECT, TASK AREA & WORK UNIT NUMBERS
14. MONITORING AGENCY NAME & ADDRESS (if different from Controlling Office)		12. REPORT DATE November 1983
		13. NUMBER OF PAGES
		15. SECURITY CLASS. (of this report) Unclassified
		15a. DECLASSIFICATION/DOWNGRADING SCHEDULE
16. DISTRIBUTION STATEMENT (of this Report)  Approved for Public Release; distribution unlimited		
17. DISTRIBUTION STATEMENT (of the abstract entered in Block 20, if different from Report)		
18. SUPPLEMENTARY NOTES		
19. KEY WORDS (Continue on reverse side if necessary and identify by block number)  Macrocycle complexes, sepulchrates, Cobalt(III)/(II) redox couples, surface-attached reactants, reaction entropies		
20. ABSTRACT (Continue on reverse side if necessary and identify by block number)		

REDOX THERMODYNAMICS OF SURFACE-BOUND REACTANTS.  
ILLUSTRATIVE BEHAVIOR OF COBALT(III)/(II) MACROBICYCLIC "CAGE"  
COMPLEXES.

J.T. Hupp, P.A. Lay\*, H.Y. Liu, W.H.F. Petri\*, A.M. Sargeson\*, and M.J. Weaver<sup>†</sup>  
Department of Chemistry, Purdue University, West Lafayette, IN 47907, USA,  
and Research School of Chemistry, Australian National University, Canberra  
ACT 2600, Australia.

The electrochemistry of surface-bound redox couples is an area of considerable current interest. In addition to their potential applications in electrocatalysis, such couples that involve mechanistically uncomplicated one-electron transfer offer opportunities for studying several fundamental aspects of heterogeneous electron-transfer processes. For example, the interpretation of electrochemical rate parameters for surface-attached reactants is especially straightforward, since these provide direct information on the energetics of the elementary electron-transfer step.

The comparison between redox thermodynamics of a given redox couple in solution and in the surface-bound state are expected to yield useful insights into the differences in the solvating environment between the interfacial region and the bulk solution. Bulk solution and surface thermodynamic behavior for two Co(III)/(II) redox couples adsorbed by different means is presented here in order to illustrate the virtues of such analyses for simple electrode reactions. The structures of these two macrobicyclic ("sarcophagine") couples,<sup>3</sup> Co(EFMEoxosar-H)<sup>2+/+</sup> and Co(diNOsar)<sup>3+/2+</sup>,<sup>4</sup> are shown in Fig. 1a and 1b, respectively. These complexes are extremely stable in both oxidation states, yielding chemically reversible one-electron transfer in a variety of solvents.<sup>5</sup> The cobalt salts Co(EFMEoxosar-H) (CF<sub>3</sub>SO<sub>3</sub>)<sub>2</sub> and Co(diNOsar) (ClO<sub>4</sub>)<sub>3</sub> used here were prepared as described in ref. 5.

---

\*Australian National University

<sup>†</sup>Author to whom correspondence should be addressed.

The  $\text{Co}(\text{EFMEoxosar-H})^{2+/+}$  couple was found to be strongly adsorbed at mercury, both from water and N-methylformamide (NMF). Cyclic voltammetric waves due almost entirely to reaction of adsorbed material were obtained by using dilute solutions of the  $\text{Co}(\text{III})$  complex (30 - 100  $\mu\text{M}$ ) together with rapid scan rates (10-200  $\text{V s}^{-1}$ ). Measurements were made at a hanging mercury drop electrode with either 0.1  $\text{M}$   $\text{KPF}_6$  or 1  $\text{M}$   $\text{NaClO}_4$  as supporting electrolyte. The electrochemical measurements utilized a PAR 173 potentiostat with a PAR 175 potential programmer, the voltammetric traces being recorded using a Nicolet Explorer I oscilloscope coupled to a Houston 2000 X-Y recorder. Cyclic voltammograms for the bulk redox couple were obtained using slower sweep rates (100-500  $\text{mV sec}^{-1}$ ) and higher bulk concentrations (ca. 1  $\text{mM}$ ). Other experimental details are given elsewhere.<sup>7</sup>

A cyclic voltammogram for the  $\text{Co}(\text{EFMEoxosar-H})^{2+/+}$  surface-bound couple in a 0.1  $\text{M}$  aqueous  $\text{KPF}_6$  is shown in Fig 2. The symmetrical shape of the voltammogram and the identical peak potentials for the anodic and cathodic waves are indicative of a reversible surface process, while the 230 mV peak width at half height can be interpreted as evidence of repulsive interactions between the adsorbed cations.<sup>8</sup> Reversible behavior persists at least to scan rates of 200  $\text{V s}^{-1}$ . Thus, a lower limit of circa.  $5 \times 10^3 \text{ s}^{-1}$  is thereby indicated for the standard rate constant,  $k_{\text{et}}^s$ , of the surface-bound couple.<sup>9</sup> Adsorption of  $\text{Co}(\text{EFMEoxosar-H})^{2+/+}$  is perhaps a surprising finding. Given the structure of the complex it seems feasible that specific adsorption occurs through chelation at the mercury surface by the enolate and ester carbonyl groups (Fig. 1a). Although somewhat speculative, this mode of surface coordination is supported by the isolation of a binuclear complex where these carbonyl groups are coordinated to  $\text{Co}(\text{en})_2^{3+}$  (en = ethylenediamine).<sup>10</sup>

A striking contrast to the simple behavior of  $\text{Co}(\text{EFME-oxosar})^{2+/+}$  is found for adsorbed  $\text{Co}(\text{diNOsar})^{3+/2+}$ . Cyclic voltammograms (as in Fig. 3) for the surface redox reaction of this complex in aqueous 1.0  $\text{M}$   $\text{NaClO}_4$  are

markedly asymmetric, exhibiting a very sharp oxidation peak and a broad reduction peak. The peak separation at a scan rate of  $10 \text{ V s}^{-1}$  is 60 mV while the anodic and cathodic peak widths at half height are 41 mV and 98 mV, respectively. The peak separation is substantially less than 60 mV at lower scan rates. A shift of the sharp anodic peak to more negative potentials occurs as the sweep rate is decreased, while the cathodic peak remains largely unaffected. The area under the reverse (cathodic) peak was generally smaller than beneath the forward (anodic) peak, especially at low sweep rates. This appears to be due to partial desorption of the more soluble Co(III) form. Stronger adsorption of the Co(II) form was also indicated from single-step chronocoulometric measurements. For both  $\text{Co}(\text{EFMEoxosar-H})^{2+/+}$  and  $\text{Co}(\text{diNOsar})^{3+/2+}$ , the peak currents vary approximately linearly with scan rate, confirming that the waves arise from surface-bound rather than bulk-phase reactant.

Adsorption of  $\text{Co}(\text{diNOsar})^{3+/2+}$  is readily detected in aqueous  $\text{NaClO}_4$ ,  $\text{NaCl}$ , and  $\text{Na}_2\text{SO}_4$  electrolytes but is absent in  $\text{KPF}_6$  media. Similar behavior is seen with  $\text{Co}(\text{sepulchrate})^{3+/2+}$ <sup>3,11</sup> and  $\text{Co}(\text{en})_3^{3+/2+}$ . All three of these couples lack ligands which would normally be expected to induce specific adsorption via surface coordination. Evidently adsorption occurs instead via "surface precipitation".<sup>12</sup> Thus, the solubility product of  $\text{Co}(\text{diNOsar})^{3+} \cdot \text{X}_3^-$ , where  $\text{X}^-$  is the supporting electrolyte anion, can be exceeded at the mercury surface even when the complex remains soluble in the bulk solution since, as a consequence of anion specific adsorption, the concentration of  $\text{ClO}_4^-$ ,  $\text{Cl}^-$  or  $\text{SO}_4^{2-}$  ions will be enhanced at the electrode surface. In addition, the diffuse-layer concentration of the positively charged complex will be increased relative to its bulk value if super-equivalent adsorption of anions occurs. The absence of specific adsorption of  $\text{Co}(\text{diNOsar})^{3+/2+}$  in  $\text{KPF}_6$  solutions provides strong support to this explanation. Thus although the

bulk solubility of the hexafluorophosphate and perchlorate salts of  $\text{Co}(\text{diNOsar})^{3+}$  are similar,  $\text{PF}_6^-$  is adsorbed only to a small extent at the mercury-aqueous interface in comparison to most other anions.<sup>13</sup>

The cyclic voltammogram in Fig. 3 closely resembles those obtained by Daum and Murray<sup>14</sup> for ferrocene polymer film electrodes. Laviron and Roullier showed that such highly asymmetric voltammograms can be obtained when charge transfer is kinetically controlled and the composite Frumkin isotherm parameters characterizing ox-ox, red-red, ox-red and transition state-ox and -red interactions have widely differing values.<sup>15</sup> Their treatment can at least formally be applied to the present case. Thus, despite the obvious chemical differences, the peculiarities of surface redox reactions of poly-(vinyl ferrocene) and of adsorbed  $\text{Co}(\text{diNOsar})^{3+/2+}$  may have a common explanation.

Although quantitative determinations of  $k_{\text{et}}^{\text{S}}$  are precluded, the quasi-reversible behavior of adsorbed  $\text{Co}(\text{diNOsar})^{3+/2+}$  indicates that this couple exhibits substantially smaller values of  $k_{\text{et}}^{\text{S}}$  than adsorbed  $\text{Co}(\text{EFMEoxosar-H})^{2+/+}$  even though the outer-sphere redox reactivities of these two couples are similar.<sup>6</sup> The abnormally sluggish kinetics for the former system may arise from structural changes in the adsorbed layer, such as anion migration, associated with electron transfer. This behavior is consistent with the present interpretation of the adsorbate as a surface precipitate since it would be expected to form a structurally ordered "ionic lattice", whose two-dimensional structure may well differ in the oxidized and reduced forms. As a caveat to other experimentalists, we note that the presence of such surface precipitation can substantially influence the values of apparent heterogeneous rate parameters for the solution reactant. Surprisingly small standard rate constants ( $\lesssim 5 \times 10^{-3} \text{ cm s}^{-1}$ ) were often obtained for  $\text{Co}(\text{diNOsar})^{2+/+}$  and other  $\text{Co}(\text{III})/(\text{II})$  couples under conditions where surface precipitation



was encountered, much faster rates generally being obtained in 0.1 M  $\text{KPF}_6$  where surface precipitation is absent. These slow rates may be due either to unfavorable double-layer effects arising from the surface precipitate or to the presence of a reaction pathway involving surface precipitation prior to electron transfer. AC polarography was found to be a sensitive method for detecting these complications, since waves due to the reaction of both adsorbed and bulk complexes are typically observed.<sup>5</sup>

In addition to comparing formal potentials for corresponding surface-bound and bulk-phase couples,  $E_a^f$  and  $E^f$  respectively, it is instructive to compare their entropic components determined from the temperature coefficients of  $E_a^f$  and  $E^f$ . We have demonstrated that the difference in absolute ionic entropies,  $\bar{S}_{\text{red}}^\circ - \bar{S}_{\text{ox}}^\circ$ , between the reduced and oxidized forms of the bulk-phase redox couple (the so-called "reaction entropy"  $\Delta S_{\text{rc}}^\circ$ ), can be obtained directly from the temperature dependence of  $E^f$  using a nonisothermal cell arrangement.<sup>7</sup> Reaction entropies provide a sensitive monitor of the changes in solvent polarization ("ordering") resulting from electron transfer.<sup>7,16-18</sup> Measurements of  $\Delta S_{\text{rc}}^\circ$  for surface-bound (or adsorbed) couples,  $\Delta S_{\text{rc,s}}^\circ$ , can provide similarly valuable information on the solvation changes induced by electron transfer within the interfacial environment.<sup>18</sup>

Table I summarizes bulk-phase and surface thermodynamic parameters for  $\text{Co}(\text{EFMEoxosar-H})^{2+}/+$  in water and NMF. The values of  $E^f$  and  $E_a^f$  were both approximated by the mean of the cathodic- and anodic-going peak potentials, and  $\Delta S_{\text{rc}}^\circ$  and  $\Delta S_{\text{rc,s}}^\circ$  determined from the temperature dependence of  $E^f$  and  $E_a^f$ , respectively, with the reference electrode held at room temperature as described in ref. 7. The reaction entropy of adsorbed  $\text{Co}(\text{diNOsar})^{3+/2+}$  is not reported, since the required values of  $E_a^f$  could not be determined with sufficient accuracy.

One interesting result is the smaller values of  $\Delta S_{\text{rc}}^\circ$  found for the surface reactions compared to the solution couples. For solution redox reactions a correlation has been found between the magnitude of  $\Delta S_{\text{rc}}^\circ$  and the

degree of "internal order" of the solvent, the smallest values being found in highly structured solvents such as water.<sup>7b,17,18</sup> A plausible interpretation of the decreases in  $\Delta S_{rc}^\circ$  accompanying adsorption is that the redox couple experiences a relatively "more structured" solvent environment at the surface than in solution. This increased structuring could be induced by orientation of the solvent at the mercury surface. It seems likely that solvent molecules thus constrained would be less able than their bulk solution counterparts to undergo the charge-induced reorientations that largely determine reaction entropies.<sup>7</sup> However, only small differences in  $\Delta S_{rc}^\circ$  have been observed between related surface-bound and bulk-solution ferrocene couples, where the redox center lies within the diffuse layer.<sup>18</sup> An alternative, more likely additional, explanation of the decreases in  $\Delta S_{rc}^\circ$  attending reactant adsorption is that the surface-bound couple is partially desolvated within the inner layer and therefore polarizes fewer solvent molecules than it would in bulk solution. In any case, it is evident that  $\text{Co}(\text{EFMEoxosar-H})^{2+/+}$  experiences a significantly different solvent environment at the electrode than in solution.

Significant differences between  $E^f$  and  $E_a^f$  are also found. These are expressed in terms of differences in reaction free energy,<sup>7b</sup>  $\Delta(\Delta G_{rc}^\circ)_{s-b}$ , between the surface and bulk redox couples, where  $\Delta(\Delta G_{rc}^\circ)_{s-b} = -F(E_a^f - E^f)$ . The corresponding entropic and enthalpic components,  $\Delta(\Delta S_{rc}^\circ)_{s-b}$  and  $\Delta(\Delta H_{rc}^\circ)_{s-b}$ , are also listed in Table I. An interesting finding is that both enthalpic and entropic factors, acting in opposing directions, are important in determining the changes in redox potential attending adsorption.

Further insights into the factors influencing reactant solvation at electrode surfaces as well as in bulk solution can be obtained by examining the changes in redox thermodynamics brought about by altering the solvent. Free energies of transfer from water to NMF,  $\Delta(\Delta G_{rc}^\circ)_{\text{NMF-H}_2\text{O}}$ , for

Co(EFME-oxosar)<sup>2+/+</sup> in both bulk and interfacial environments, along with related data for some structurally related cobalt complexes, are shown in Table II. These were calculated from the formal potentials in the two solvents on the basis of the TATB assumption as described in ref. 7b. The uniformly positive transfer free energies are consistent with the greater solvent donicity for NMF than water.<sup>19</sup> Thus the stronger donor-acceptor interactions between the NMF solvent and the amine hydrogens should yield negative transfer free energies for both Co(III) and Co(II) forms, but to a greater extent with the former, yielding positive values of  $\Delta(\Delta G_{rc}^{\circ})_{\text{NMF-H}_2\text{O}}$ .<sup>7b</sup> It is interesting to note that  $\Delta(\Delta G_{rc}^{\circ})_{\text{NMF-H}_2\text{O}}$  for Co(EFMEoxosar-H)<sup>2+/+</sup> is somewhat larger at the electrode surface than in solution. A detailed examination of transfer free energies between a variety of solvents<sup>5b</sup> for Co(EFMEoxosar-H)<sup>2+/+</sup> in solution indicates that the values are influenced by solvent-acceptor interactions with the electron-rich enolate group. Since water is a better electron acceptor than NMF,<sup>19</sup> electron-pair donation from a ligand to the solvent will lead to less positive values of  $\Delta(\Delta G_{rc}^{\circ})_{\text{NMF-H}_2\text{O}}$ . With adsorbed Co(EFMEoxosar-H)<sup>2+/+</sup> electron-pair donation to the solvent cannot occur if, as suggested above, the oxygens are bound to the mercury surface. This mode of surface coordination can therefore account for the larger values of  $\Delta(\Delta G_{rc}^{\circ})_{\text{NMF-H}_2\text{O}}$ .

These results demonstrate that substantial differences in the redox thermodynamics of surface-bound and bulk-phase redox couples can arise which are attributable to the influence of the electrode surface upon the reactant-solvent interactions. The identification of such effects is greatly facilitated by separating the formal potential shifts into entropic and enthalpic components. Systematic studies along these lines for simple one-electron redox couples should not only provide valuable information on the nature of ionic solvation at electrode surfaces but may

also shed light on the influence of the interfacial environment on the kinetics of heterogeneous electron transfer.

Acknowledgements

P.A.L. gratefully acknowledges support from a CSIRO fellowship. The research program of M.J.W. was supported in part by the Air Force of Scientific Research and the Office of Naval Research.

# References

1. For reviews, see R.W. Murray, *Acc. Chem. Res.*, **13**, 135 (1980);  
K.D. Snell, A.G. Keenan, *Chem. Soc. Rev.*, **8**, 259 (1979);  
W.R. Heineman, P.T. Kissinger, *Anal. Chem.*, **52**, 138R (1980);  
M.D. Ryan, G.S. Wilson, *Anal. Chem.*, **54**, 20R (1982).
2. J.T. Hupp, M.J. Weaver, *J. Electroanal. Chem.*, **143**, 43 (1983).
3. A.M. Sargeson, *Chem. Brit.*, **15**, 23 (1979).
4.  $[\text{Co}(\text{EFMEoxosar-H})]^{2+} = [1\text{-carboxyethyl-8-methyl-2-oxo-3,6,10,13,16,19-hexaazabicyclo[6.6.6]icosanato(1-)}]\text{cobalt(III)}$ ;  $[\text{Co}(\text{diNOsar})]^{3+} = [1,8\text{-dinitro-3,6,10,13,16,19-hexaazabicyclo[6.6.6]icosane}]\text{cobalt(III)}$ .
5. (a) A.M. Bond, G.A. Lawrence, P.A. Lay, A.M. Sargeson *Inorg. Chem.*, **1983**, 22, 2010; I.I. Creaser, A.M. Sargeson, A.W. Zanell *Inorg. Chem.*, in press;  
(b) P.A. Lay, J.T. Hupp, A.M. Sargeson, M.J. Weaver in preparation.
6. R.J. Geue, J. Mac B. Harrowfield, T.W. Hambley, A.M. Sargeson, M.R. Snow, *J. Am. Chem. Soc.*, submitted; P.A. Lay, W. Petri, A.M. Sargeson, M.R. Snow, to be published.
7. (a) E.L. Yee, R.J. Cave, K.L. Guyer, P.D. Tyma, M.J. Weaver, *J. Am. Chem. Soc.*, **101**, 1131 (1979); (b) S. Sahami, M.J. Weaver, *J. Electroanal. Chem.*, **122**, 155, 171 (1981).
8. E. Laviron, *J. Electroanal. Chem.*, **100**, 263 (1979).
9. H. Angerstein-Kozłowska, B.E. Conway, *J. Electroanal. Chem.*, **95**, 1 (1979); E. Laviron, *J. Electroanal. Chem.*, **97**, 135 (1979).
10. W. Petri, A.M. Sargeson, unpublished results.
11. Sepulchrates = 1,3,5,8,10,13,16,19-octaazabicyclo[6.6.6]icosane.
12. For example, see H.B. Herman, R.L. McNeely, P. Surana, C.M. Elliott, R.W. Murray, *Anal. Chem.*, **46**, 1258 (1974).
13. L.M. Baugh, R. Parsons, *J. Electroanal. Chem.*, **40**, 407 (1972).
14. P. Daum, R.W. Murray, *J. Electroanal. Chem.*, **103**, 289 (1979).
15. E. Laviron, L. Roullier, *J. Electroanal. Chem.*, **115**, 65 (1980).
16. E.L. Yee, M.J. Weaver, *Inorg. Chem.*, **19**, 1077 (1980).
17. S. Sahami, M.J. Weaver, *J. Sol. Chem.*, **10**, 199 (1981).
18. J.T. Hupp, M.J. Weaver, submitted to *J. Electrochem. Soc.*
19. V. Gutmann, "The Donor-Acceptor Approach to Molecular Interactions", Plenum Press, New York, 1978, Chapter 2.

TABLE I. Comparison of thermodynamics of  $\text{Co}(\text{EFMExoxosar-H})^{2+/+}$  and  $\text{Co}(\text{diNOSar})^{3+/2+}$  in bulk solution and surface-bound environments.

Couple <sup>a</sup>	Environment <sup>b</sup>	$E^f$ c mv vs $F_c/F_c$	$\Delta S_{rc}^d$ J deg <sup>-1</sup> mol <sup>-1</sup>	$\Delta(\Delta G_{rc}^\circ)^e$ kJ mol <sup>-1</sup> s-b	$T\Delta(\Delta S_{rc}^\circ)^f$ kJ mol <sup>-1</sup> s-b	$\Delta(\Delta H_{rc}^\circ)^g$ kJ mol <sup>-1</sup> s-b
$\text{Co}(\text{EFMExoxosar-H})^{2+/+}$	surface- $\text{H}_2\text{O}$	-824 <sup>h,i</sup>	21±5	-11.5	-2.5	-14.0
$\text{Co}(\text{EFMExoxosar-H})^{2+/+}$	bulk- $\text{H}_2\text{O}$	-942 <sup>h</sup>	29±4			
$\text{Co}(\text{EFMExoxosar-H})^{2+/+}$	surface-NMF	-1227 <sup>h</sup>	67±5	2.0	-7.5	-5.5
$\text{Co}(\text{EFMExoxosar-H})^{2+/+}$	bulk-NMF	-1206 <sup>h</sup>	92±4			
$\text{Co}(\text{diNOSar})^{3+/2+}$	surface- $\text{H}_2\text{O}$	~370 <sup>i,j</sup>	---			
$\text{Co}(\text{diNOSar})^{3+/2+}$	bulk- $\text{H}_2\text{O}$	-379 <sup>i</sup>	105±4	-0.9	---	---

Notes to Table I

<sup>a</sup>For structures of redox couples, see Fig 1.

<sup>b</sup>Surface was mercury in each case.

<sup>c</sup>Formal potential for bulk or surface-bound redox couple versus ferricinium-ferrocene couple in same solvent; determined by cyclic voltammetry as described in text. Usually reproducible to  $\pm 2$  mV.

<sup>d</sup>Reaction entropy for bulk or surface-bound couple, as determined from  $\Delta S^\circ = F(dE_{ni}^f/dT)$ , where  $E_{ni}^f$  is the formal potential measured using a nonisothermal cell arrangement (See ref. 7 for details).

<sup>e</sup>Free energy of transfer of redox couple from bulk to surface-bound environment, determined from  $\Delta(\Delta G_{rc}^\circ)_{s-b} = -F(E_a^f - E^f)$ , where  $E_a^f$  and  $E^f$  are formal potentials in surface and bulk environments.

<sup>f</sup>Entropic component of  $\Delta(\Delta G_{rc}^\circ)_{s-b}$ , determined from  $T\Delta(\Delta S_{rc}^\circ)_{s-b} = T(\Delta S_{rc,s}^\circ - \Delta S_{rc}^\circ)$ , where  $\Delta S_{rc,s}^\circ$  and  $\Delta S_{rc}^\circ$  are reaction entropies of surface-bound and bulk redox couples, respectively.

<sup>g</sup>Enthalpic component of  $\Delta(\Delta G_{rc}^\circ)_{s-b}$ , determined from  $\Delta(\Delta H_{rc}^\circ)_{s-b} = \Delta(\Delta G_{rc}^\circ)_{s-b} + T\Delta(\Delta S_{rc}^\circ)_{s-b}$ .

<sup>h</sup>Determined in 0.1 M KPF<sub>6</sub>

<sup>i</sup>Determined in 1 M NaClO<sub>4</sub>

<sup>j</sup>Estimated by extrapolating measured  $E_{1/2}$  to zero voltammetric sweep rate.

TABLE II. Free energies of transfer,  $\Delta(\Delta G_{rc}^\circ)^a_{\text{NMF-H}_2\text{O}}$ , of Co(III)/(II) redox couples in bulk and surface-bound environments from water to N-methylformamide.

Redox Couple	Environment	$\Delta(\Delta G_{rc}^\circ)^a_{\text{NMF-H}_2\text{O}}$ kJ mol <sup>-1</sup>
Co(EFMEoxosar-H) <sup>2+/+</sup> <sup>d</sup>	bulk	17.0 <sup>b</sup>
Co(EFMEoxosar-H) <sup>2+/+</sup> <sup>d</sup>	mercury surface	30.5 <sup>b</sup>
Co(diNOsar) <sup>3+/2+</sup> <sup>d</sup>	bulk	24.0 <sup>b</sup>
Co(sepulchrates) <sup>3+/2+</sup> <sup>e</sup>	bulk	26.5 <sup>c</sup>
Co(en) <sub>3</sub> <sup>3+/2+</sup> <sup>f</sup>	bulk	23.5 <sup>c</sup>

<sup>a</sup>Values of  $\Delta(\Delta G_{rc}^\circ)_{\text{NMF-H}_2\text{O}}$  determined from measured formal potentials in H<sub>2</sub>O and NMF, using TATB assumption as outlined in ref. 7b.

<sup>b</sup>Determined from data in Table I.

<sup>c</sup>From data in ref. 7b.

<sup>d</sup>For structures, see Figure 1.

<sup>e</sup>See ref. 11.

<sup>f</sup>en = ethylenediamine.



### Figure Captions

Figure 1. (a) Structure of  $\text{Co}(\text{EFMEoxosar-H})^{2+}$ .

(b) Structure of  $\text{Co}(\text{diNOsar})^{3+}$ .

Figure 2. Cyclic voltammogram for surface-bound  $\text{Co}(\text{EFMEoxosar-H})^{2+/+}$  at mercury in aqueous  $1.0 \text{ M NaClO}_4$  at  $25^\circ\text{C}$ . Reactant concentration =  $50 \text{ }\mu\text{M}$ . Scan rate =  $10 \text{ V s}^{-1}$ .

Figure 3. Cyclic voltammogram of precipitated  $\text{Co}(\text{diNOsar})^{3+/2+}$  at mercury in aqueous  $1.0 \text{ M NaClO}_4$  at  $25^\circ\text{C}$ . Reactant concentration =  $50 \text{ }\mu\text{M}$ . Scan rate =  $20 \text{ V s}^{-1}$ .

DA  
FILM